Optimized growth of lattice-matched $In_xAl_{1-x}N$/GaN heterostructures by molecular beam epitaxy

S. Schmult,[a] T. Siegrist, A. M. Sergent, and M. J. Manfra[b]
Bell Laboratories, Lucent Technologies, 600 Mountain Avenue, Murray Hill, New Jersey 07974

R. J. Molnar
MIT Lincoln Laboratory, 244 Wood St., Lexington, Massachusetts 02420

(Received 19 October 2006; accepted 8 December 2006; published online 12 January 2007)

The authors present a systematic study on the growth of the ternary compound $In_xAl_{1-x}N$ by molecular beam epitaxy. This work concentrates on In mole fractions x around 0.17, as this composition is in-plane lattice matched to GaN. At a growth temperature of 540 °C, high quality material was obtained using a total metal to nitrogen flux ratio of ~1. Using these growth parameters, high quality GaN/InAlN superlattices were obtained without growth interruptions.
 [DOI: 10.1063/1.2430940]

A fundamental problem for the growth of group III-nitride heterostructures is the lattice constant mismatch between the binary compounds GaN, AlN, and InN. This mismatch in multilayered structures results in strain, and potentially crack formation, that deteriorates the performance of devices. Recent interest has focused on the ternary compound $In_xAl_{1-x}N$, which is in-plane lattice matched to GaN for $x \approx 0.17$.[1] To date, state-of-the-art optoelectronic devices utilizing lattice-matched InAlN/GaN multilayers are realized by metal organic vapor phase epitaxy (MOVPE) exclusively.[2–4] There have been a few reports of molecular beam epitaxy (MBE) growth of InAlN bulk layers[5] and InAlN/GaN single heterojunctions for high power electronic applications.[6–8] The development of MBE grown lattice-matched multilayers offers the potential for novel optoelectronic devices as well as the investigation of interesting physical phenomena such as strong light-matter coupling[9] and solid state Bose-Einstein condensation.[10]

In this work we show that high quality, lattice-matched, InAlN/GaN multilayers can be obtained using MBE. It is found that below a growth temperature of 550 °C indium can be reproducibly incorporated at mole fractions between 0.1 and 0.2. Optimizing the growth conditions involves regulating the Al to In flux ratio for a given nitrogen flux such that the growth occurs near stoichiometric conditions (i.e., the ratio between the total metal flux and the flux of the active nitrogen is 1). Our experimental results demonstrate that InAlN/GaN multilayers can be fabricated by MBE in an uninterrupted growth run, yielding high structural quality and sharp interfaces as confirmed by high resolution x-ray diffraction (HRXRD).

The samples are grown by plasma assisted MBE on thick *c*-axis oriented 2 in. GaN templates prepared by hydride vapor phase epitaxy (HVPE). Active nitrogen was supplied by a radio-frequency plasma source with power set to 400 W and a nitrogen flow rate set to 0.50 SCCM (SCCM denotes cubic centimeter per minute at STP). In this work a constant In beam equivalent pressure (BEP) of 1.3×10^{-8} Torr was used. The growth temperature was set to 540 °C, as measured with optical pyrometry. A growth temperature below 550 °C had to be used to incorporate an appreciable amount of In. The structural quality of the samples was determined by HRXRD scans around the (0002) Bragg condition of GaN in ω-2θ geometry using the Cu $K\alpha$ line ($\lambda = 1.5406$ Å) and by rocking curve scans. The indexing of the hexagonal lattice follows the notation $(hk\overline{(h+k)}l)$.

Having established the growth temperature and In beam flux necessary to incorporate In into the lattice, the Al BEP has been varied between 0.5 and 4.5×10^{-8} Torr. In our study, the crystal quality was found to be strongly dependent on the Al to In flux ratio. For low Al BEPs, the surface of the sample was covered with excess In, and the reflection high energy electron diffraction (RHEED) pattern during growth was dim. As we increased the Al flux the crystal quality improved dramatically. The growth rate also increased, indicating that the growth was limited by the Al supply. Optimal growth conditions were observed at an Al beam BEP of 2.8×10^{-8} Torr, represented by bright streaky RHEED pattern during the growth (indicative of smooth two-dimensional growth), no excess metal on the sample surface, and the smallest full width at half maximum (FWHM) of 190 arc sec extracted from the ω-2θ scan (Fig. 1). The sample surface is smooth when inspected under an optical microscope with 80× magnification in the Normarski contrast mode. The FWHM of the InAlN peaks extracted from the (0002) HRXRD scans $[\Delta(\omega\text{-}2\theta)]$ and the rocking curves $[\Delta(\omega)]$ are summarized in Fig. 2. For the highest Al BEP of 4.5×10^{-8} Torr, the RHEED pattern became very spotty after few minutes of deposition, indicating the onset of three-dimensional growth. In addition, the sample surface was covered with excess aluminum and the FWHM of the InAlN (0002) and rocking curve scans become wider again, indicating deterioration of the material quality. The rocking curve FWHM values for the substrate and the InAlN peaks are similar, suggesting that the quality of the substrate material limits the InAlN structural quality. The numbers presented with the data points in Fig. 2 denote the In mole fraction in each sample. The In mole fraction varies insignificantly over the entire wafer and can be extracted with an absolute certainty of 0.01. The HRXRD spectrum displayed in Fig. 1 shows the entire θ range from 15.5° to 18.5°, no peaks are identified except those corresponding to GaN and InAlN. We do not observe metal segregation or phase separation in the

[a]Electronic mail: stefan.schmult@gmail.com
[b]Electronic mail: manfra@alcatel-lucent.com

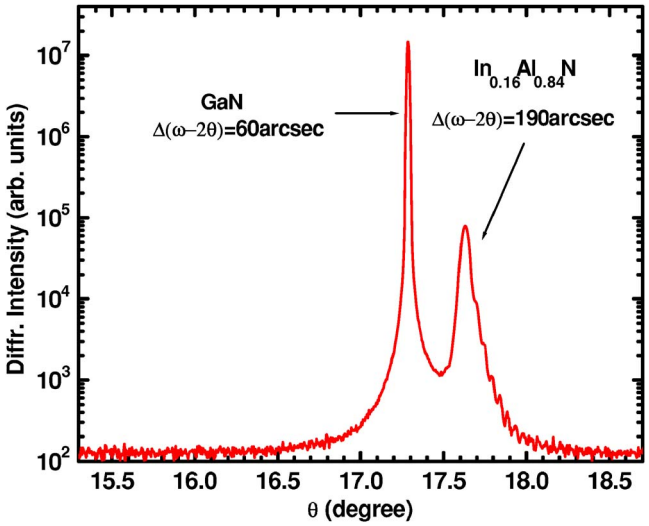

FIG. 1. HRXRD ω-2θ scan of an ≈100 nm thick $In_{0.16}Al_{0.84}N$ layer grown on 75 μm HVPE GaN. The FWHM of the InAlN peak is 190 arc sec. The peak positions of the different materials are marked for clarity. The scan range includes the (0002) Bragg conditions for InN (≈15.7°) and AlN (≈18.0°). Since only the peaks corresponding to GaN and InAlN are visible possible phase separation can be excluded.

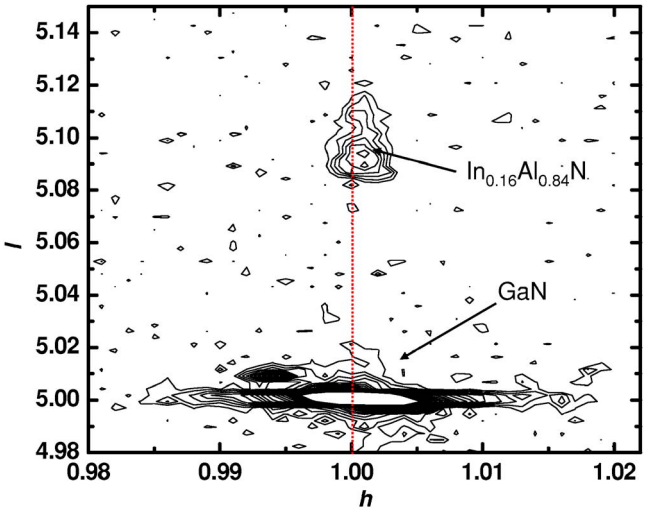

FIG. 3. Reciprocal lattice map around the asymmetric GaN ($10\bar{1}5$) reflex of the sample discussed in Fig. 1. The positions of the GaN and the $In_{0.16}Al_{0.84}N$ peaks are indicated. Beside these two materials, no other reflections can be identified. The vertical dashed line is a guide to highlight the region of in-plane lattice match.

x-ray data.[7] Thin film interference in the ω-2θ scans is observed for samples with the lowest FWHM values, allowing the extraction of the InAlN top layer thicknesses. The resulting growth rates are given in Fig. 2. Under optimal growth conditions a growth rate of 130 nm/h is obtained.

To acquire information about the degree of in-plane lattice mismatch, reciprocal lattice scans were carried out around the asymmetric GaN ($10\bar{1}5$) reflex. For the sample discussed in Fig. 1, the reciprocal lattice mapping is shown in Fig. 3. The number h represents the in-plane lattice vector. Indeed, the lattice mismatch between the GaN substrate and the 100 nm thick InAlN is smaller than 0.1%. Furthermore, no reflections other than those corresponding to GaN and InAlN can be identified, further indicating that we have grown homogeneous material without phase separation.

For a further evaluation of the structural properties of heterostructures, short period superlattices were grown. These structures allow us to assess the quality of the InAlN/GaN interfaces as a prelude to more complex optical structures including distributed Bragg reflectors and microcavities. For the growth of a ten period $GaN/In_{0.15}Al_{0.85}N$ superlattice (7.1 nm/5.9 nm) the optimized growth conditions described above were used. Unlike MOVPE growth[2] all layers are grown at a single substrate temperature and no growth interruptions are used. The (0002) ω-2θ XRD scan is presented in Fig. 4. Sharp, intense, satellite peaks are visible, as well as interface fringes, indicative of the sample's high crystalline quality and abrupt interfaces. This result points out the possibility of growing GaN/InAlN heterostructures

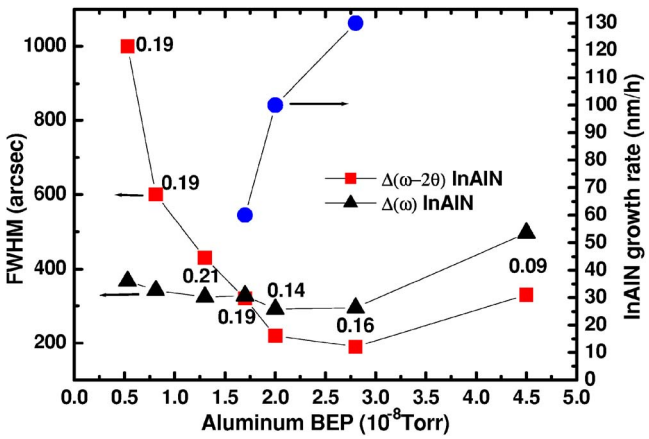

FIG. 2. Full widths at half maximum (FWHMs) of the InAlN (0002) peaks and rocking curves and the growth rate of InAlN as a function of the Al BEP. The lines are a guide for the eye. Over the entire metal-lean range the rocking curve values do not change significantly, whereas the width in the ω-2θ scans decreases dramatically with increasing aluminum BEP. Thin film interference is clearly observed in the Al BEP regime around 2.5×10^{-8} Torr, allowing for a simple extraction of the growth rate. The numbers at the data points correspond to the indium mole fraction. The growth temperature for all samples was 540 °C and the In BEP was 1.3×10^{-8} Torr. The growth rates of InAlN are extracted from the thin film interferences in the ω-2θ scans.

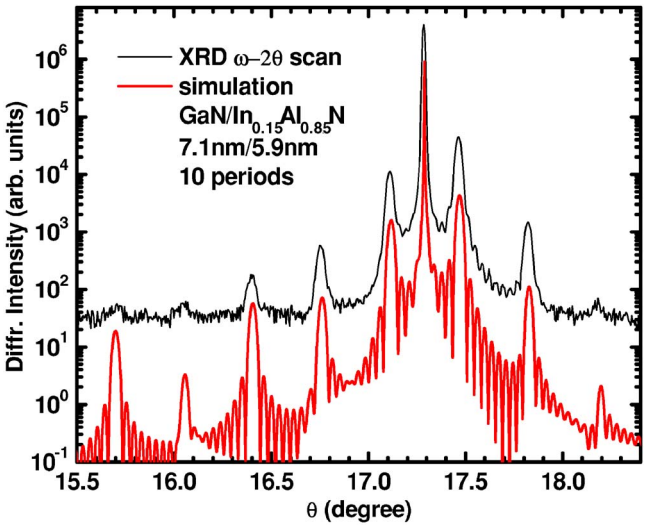

FIG. 4. HRXRD scan around the (0002) GaN reflex of a ten period $GaN/In_{0.15}Al_{0.85}N$ superlattice grown on 115 μm GaN and simulated spectrum of a ten period $GaN/In_{0.15}Al_{0.85}N$ (7.1 nm/5.9 nm) structure. Sharp and intense higher order superlattice satellite peaks and interface interferences are resolved.

without changing the growth conditions for the different layers. The simulated spectrum in Fig. 4 is based on the dynamical scattering theory using a commercial simulator.[11]

In conclusion, we demonstrate the MBE growth of $In_xAl_{1-x}N$ around the In mole fraction $x=0.17$, where the InAlN is in-plane latticed matched to GaN. At a metal to nitrogen flux ratio close to 1, the smallest values of the FWHM for both rocking curve and ω-2θ scans are obtained. Short period GaN/InAlN superlattices show out to fifth order satellite peaks and exhibit clear interface interferences in ω-2θ scans, confirming the high interface quality inside the heterostructure.

One of the authors (S.S.) thanks Hock Ng, Loren Pfeiffer, and Ken West for fruitful discussions and support. The Lincoln Laboratory portion of this work was sponsored by the United States Air Force under Air Force Contract No. FA8721-05-C-0002. The opinions, interpretations, conclusions, and recommendations are those of the authors and are not necessarily endorsed by the United States Government.

[1] K. Lorenz, N. Franco, E. Alves, I. M. Watson, R. W. Martin, and K. P. O'Donnell, Phys. Rev. Lett. **97**, 085501 (2006).
[2] J.-F. Carlin and M. Ilegems, Appl. Phys. Lett. **83**, 668 (2003).
[3] J.-F. Carlin, J. Dorsaz, E. Feltin, R. Butté, N. Grandjean, M. Ilegems, and M. Laügt, Appl. Phys. Lett. **86**, 031107 (2005).
[4] J. Dorsaz, J.-F. Carlin, S. Gradecak, and M. Ilegems, J. Appl. Phys. **97**, 084505 (2005).
[5] M. J. Lukitsch, Y. V. Danylyuk, V. M. Naik, C. Huang, G. W. Auner, and L. Rimai, Appl. Phys. Lett. **79**, 632 (2001).
[6] M. Higashiwaki and T. Matsui, Jpn. J. Appl. Phys., Part 2 **43**, L768 (2004).
[7] D. S. Katzer, D. F. Storm, S. C. Binari, and B. V. Shanabrook, J. Vac. Sci. Technol. B **23**, 1204 (2005).
[8] M. Higashiwaki, T. Mimura, and T. Matsui, Jpn. J. Appl. Phys., Part 2 **45**, L843 (2006).
[9] C. Weisbuch, M. Nishioka, A. Ishikawa, and Y. Arakawa, Phys. Rev. Lett. **69**, 3314 (1992).
[10] J. Kasprzak, M. Richard, S. Kundermann, A. Baas, P. Jeambrun, J. M. J. Kelling, F. M. Marchetti, M. H. Szymanska, R. Andre, J. L. Staehli, V. Savona, P. B. Littlewood, B. Deveaud, and Le Si Dang, Nature (London) **443**, 409 (2006).
[11] HRXRD for DIFFRACPLUS, Version 1.0, Bruker AXS GmbH, 1995–1999.